A Periodically Active Pulsar Giving Insight into Magnetospheric Physics

M. Kramer, A. G. Lyne, J. T. O'Brien, C. A. Jordan, D. R. Lorimer

PSR B1931+24 (J1933+2421) behaves as an ordinary isolated radio pulsar during active phases that are 5 to 10 days long. However, when the radio emission ceases, it switches off in less than 10 seconds and remains undetectable for the next 25 to 35 days, then switches on again. This pattern repeats quasi-periodically. The origin of this behavior is unclear. Even more remarkably, the pulsar rotation slows down 50% faster when it is on than when it is off. This indicates a massive increase in magnetospheric currents when the pulsar switches on, proving that pulsar wind plays a substantial role in pulsar spin-down. This allows us, for the first time, to estimate the magnetospheric currents in a pulsar magnetosphere during the occurrence of radio emission.

Pulsar radio emission is generally understood in terms of beams of coherent plasma radiation from highly relativistic particles above the magnetic pole of a rotating neutron star, producing pulses as the beam crosses Earth. However, there is no satisfactory theory that explains the radio emission or even the magnetospheric conditions that determine whether a neutron star emits at radio wavelengths. Observationally, the typical active lifetime of a radio pulsar is estimated to be about 10 million years, during which, on long time scales, pulsar emission is essentially steady (*1*). It was therefore surprising when a unique activity pattern was found for the pulsar PSR B1931+24 (also known as J1933+2421) during routine pulsar timing observations with the 76-m Lovell Telescope at the Jodrell Bank Observatory in the United Kingdom.

The pulsar had been considered to be a seemingly ordinary pulsar, with a spin period of 813 ms (*2*) and a typical rotational frequency derivative of $\dot{\nu} = -12.2 \times 10^{-15}$ Hz s^{-1} (Table 1) (*3*). It was noted that it exhibits considerable short-term rotational instabilities intrinsic to the pulsar, known as timing noise, but shows no evidence indicating the presence of any stellar companion. It became clear a few years ago that the pulsar was not detected in many of the regular observations and that the flux density distribution was bimodal, the pulsar being either on or off. Figure 1 shows the best-sampled data span, which covers a 20-month period between 1999 and 2001 and demonstrates the quasi-periodic pattern of the on/off sequences. The power spectrum of the data reveals a strong ~35-day periodicity with two further harmonics, which reflect the duty cycle of the switching pattern (Fig. 1). Studying a much longer time series from 1998 to 2005, including some intervals of less densely sampled data, we find that the periodicities are persistent but slowly vary with time over a period ranging from 30 to 40 days. No other known pulsar behaves this way.

To investigate the nature of the variations, we examined the rotation rate of the pulsar over a 160-day period (Fig. 2A). The variation is dominated by a decrease in rotational frequency, which is typical for pulsars. However, inspection of the longer sequences of the available data on the on phases in the diagram reveals that the rate of decrease is even more rapid during these phases, indicating values of the rotational frequency first derivative that are higher than the average value. This suggests a simple model in which the frequency derivative has different values during the off and on phases. Such a model accurately describes the short-term timing variations that are seen relative to a simple long-term slowdown model (Fig. 2B). Over the 160-day period shown, the pulsar was monitored almost daily, so that the switching times were well defined, and a model could be fitted to the data with good precision. The addition of a single extra parameter (that is, two values of the frequency derivative rather than one) reduced the timing residuals by a factor of 20 and provides an entirely satisfactory description of the data. A similar fitting procedure was applied to other well-sampled sections of the data and produced consistent model parameters (Table 1), giving values for the rotational frequency derivatives of $\dot{\nu}_{\rm off} = -10.8(2) \times 10^{-15}$ Hz s^{-1} and $\dot{\nu}_{\rm on} = -16.3(4) \times 10^{-15}$ Hz s^{-1}. These values indicate that there is an ~50% increase in spin-down rate of the neutron star when the pulsar is on.

The observed quasi-periodicity in pulsar activity and its time scale have never been seen before as a pulsar emission phenomenon and are accompanied by massive changes in the rotational slowdown rate. This raises a number of questions. Why does the emission switch on and off? Why is the activity quasi-periodic? Why is the pulsar spinning down faster when it is on?

On the shortest, pulse-to-pulse time scales, intrinsic flux density variations are often observed in pulsar radio emission. The most extreme case is displayed by a small group of pulsars that are known to exhibit "nulls" in their emission; that is, the random onset of a sudden obvious lack of pulsar emission, typically lasting between one and a few dozen pulsar rotation periods (*4*). An acceptable explanation for such nulling, which appears to be the complete failure of the radiation mechanism, is still missing. This nulling previously represented the longest known time scales for an intrinsic disappearance of pulsar emission. The facts that the off periods of PSR B1931+24 are five orders of magnitude

Table 1. Observed and derived parameters of PSR B1931+24. Standard (1σ) errors are given in parentheses after the values and are in units of the least significant digit. The distance is estimated from the dispersion measure and a model for the interstellar free electron distribution (*14*). Definitions for characteristic age, surface magnetic field, and spin-down luminosity can be found in (*5*).

Parameter	Value
Right ascension (J2000)	$19^h33^m37^s.832(14)$
Declination (J2000)	+24°36′39″.6(4)
Epoch of frequency (modified Julian day)	50629.0
Rotational frequency ν (Hz)	1.2289688061(1)
Rotational frequency derivative $\dot{\nu}$ (Hz s^{-1})	$-12.2488(10) \times 10^{-15}$
Rotational frequency derivative on $\dot{\nu}_{\rm on}$ (Hz s^{-1})	$-16.3(4) \times 10^{-15}$
Rotational frequency derivative off $\dot{\nu}_{\rm off}$ (Hz s^{-1})	$-10.8(2) \times 10^{-15}$
Dispersion measure DM (cm^{-3} pc)	106.03(6)
Flux density during on phases at 1390 MHz (μJy)	1000(300)
Flux density during off phases at 1390 MHz (μJy)	≤2
Flux density during on phases at 430 MHz (μJy)	7500(1500)
Flux density during off phases at 430 MHz (μJy)	≤40
Active duty cycle (%)	19(5)
Characteristic age τ (million years)	1.6
Surface magnetic field strength B (T)	2.6×10^8
Spin-down luminosity $\dot{E}$ (W)	5.9×10^{25}
Distance (kpc)	~4.6

Jodrell Bank Observatory, University of Manchester, Macclesfield, SK11 9DL, UK.

longer than typical nulling periods, that the activity pattern is quasi-periodic, and that not a single null has been observed during on periods strongly suggest that the phenomenon found here is different from nulling.

The approximate 35-day period might be attributed to free precession, although we find no evidence of expected (*5*) profile changes. Although switches between states are rare events, we have been able to observe one switch from on to off that occurred within 10 s, the time resolution being limited by the signal-to-noise ratio of the observations. The sudden change and the quasi-periodicity point toward a relaxation oscillation of unknown nature within the pulsar system, rather than precession.

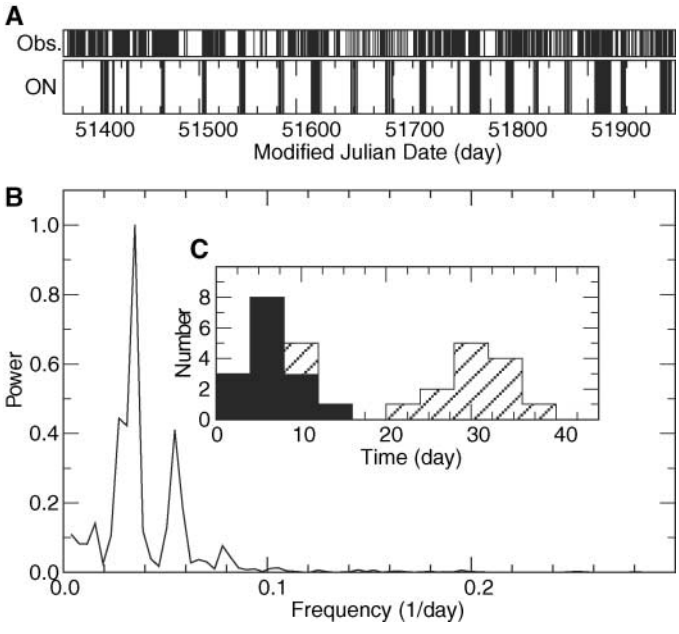

Fig. 1. Time variation of the radio emission of PSR B1931+24. During the on phases, the pulsar is easy to detect and has the stable long-term intrinsic flux density associated with most normal pulsars. Since 1998, the pulsar has been observed as frequently as twice a day. (**A**) A typical sequence of observations covering a 20-month interval is indicated by the black lines. It shows, respectively, the times of observation and the times when PSR B1931+24 was on. It is clear that the pulsar is not visible for ~80% of the time. (**B**) The appearance of the pulsar is quasi-periodic in nature, demonstrated by the power spectrum of the intensity obtained from the Fourier transform of the autocorrelation function of the mean pulse flux density obtained over the same 20-month interval. (**C**) Histograms of the durations of the on (solid) and off (hatched) phases. In off phases, integration over several weeks shows that any pulsed signal has a mean flux density of less than than 2 μJy at 1400 MHz (1 Jy = 10^{-26} W m^{-2} Hz^{-1}). A deep observation with the Arecibo telescope on Puerto Rico provides an upper flux density limit of 40 μJy at 430 MHz. Simultaneous observations at frequencies between 430 and 1400 MHz show that the presence or absence of radio emission is a broadband phenomenon.

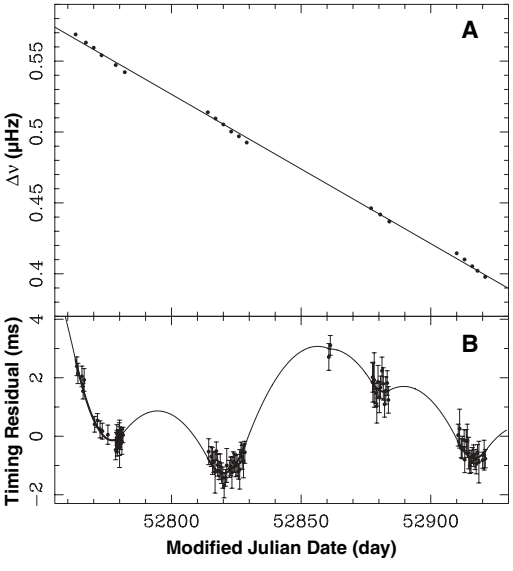

Fig. 2. Variation of the rotational frequency of PSR B1931+24. (**A**) Evolution of the rotational frequency over a 160-day period. The errors in the measurement of the data points are smaller than the size of the symbols. The variation is dominated by the long-term spin-down: a gradual decrease in rotational frequency. The best-fit straight line through the points is shown, representing a frequency derivative of $\dot{\nu} = -12.2 \times 10^{-15}$ Hz s^{-1}. However, an inspection of the data reveals that, when the pulsar is on, the slope and hence the magnitude of the derivative are even greater. This suggests a model in which the frequency derivative has different values during the off and on periods. (**B**) Examining this possibility more closely, timing residuals, which are the differences between the observed pulse arrival times and those derived from a simple long-term slowdown model (Table 1), show substantial short-term variations. Over the period covered by this figure, the pulsar was monitored almost daily, so that the off and on periods were well defined and the model described above could be fitted to the data with good precision. The fitted model is shown as a continuous line overlying the data points and clearly describes the data very well.

What can cause the radio emission to cut off so quickly? The energy associated with the radio emission from pulsars accounts for only a very small fraction of the pulsar's slowdown energy, which may suggest that the disappearance of radiation is simply due to the failure of the coherence condition in the emission process (*6*). However, in that case, the long time scales of millions of pulsar rotations are hard to understand. One alternative explanation is that there is a more global failure of charged particle currents in the magnetosphere.

The large changes in slowdown rate that accompany the changes in radio emission can also be explained by the presence or absence of a plasma whose current flow provides an additional braking torque on the neutron star. In this model, the open field lines above the magnetic pole become depleted of charged radiating particles during the off phases when the rotational slowdown, $\dot{\nu}_{off}$, is caused by a torque dominated by magnetic dipole radiation (*7*, *8*). When the pulsar is on, the decrease in rotational frequency, $\dot{\nu}_{on}$, is enhanced by an additional torque provided by the outflowing plasma, $T \sim \frac{2}{3c} I_{pc} B_0 R_{pc}^2$, where B_0 is the dipole magnetic field at the neutron star surface and $I_{pc} \sim \pi R_{pc}^2 \rho c$ is the electric current along the field lines crossing the polar cap, having radius of R_{pc} (*9*). [In order to be consistent with existing literature such as (*9*), we quote formulas in centimeter-gram-second units but refer to numerical values in SI units.] The charge density of the current can be estimated from the difference in loss in rotational energy during the on and off phases. When the pulsar is on, the observed energy loss, $\dot{E}_{on} = 4\pi^2 I \nu \dot{\nu}_{on}$, is the result of the sum of the magnetic dipole braking as seen during the off phases, $\dot{E}_{off} = 4\pi^2 I \nu \dot{\nu}_{off}$, and the energy loss caused by the outflowing current, $\dot{E}_{wind} = 2\pi T \nu$; that is, $\dot{E}_{on} = \dot{E}_{off} + \dot{E}_{wind}$, where I is the moment of inertia of the neutron star. From the difference in spin-down rates between off and on phases, $\Delta\dot{\nu} = \dot{\nu}_{off} - \dot{\nu}_{on}$, we can therefore calculate the charge density $\rho = 3I\Delta\dot{\nu}/R_{pc}^4 B_0$ by computing the magnetic field $B_0 = 3.2 \times 10^{15} \sqrt{-\dot{\nu}_{OFF}/\nu^3}$ Tesla and the polar cap radius $R_P = \sqrt{2\pi R^3 \nu / c}$ for a neutron star with radius R = 10 km and a moment of inertia of $I = 10^{38}$ kg m^2 (*10*). We find that the plasma current that is associated with radio emission carries a charge density of $\rho = 0.034$ C m^{-3}. This is remarkably close to the charge density $\rho_{GJ} = B_0 \nu / c$ in the Goldreich-Julian model of a pulsar magnetosphere (*11*); that is, $\rho_{GJ} = 0.033$ C m^{-3}.

Such charge density is sufficient to explain the change in the neutron star torque, but it is not clear what determines the long time scales or what could be responsible for suddenly changing the plasma flow in the magnetosphere. In that respect, understanding the cessation of radiation

that we see in PSR B1931+24 may ultimately also help us to understand ordinary nulling. Whatever the cause is, it is conceivable that the onset of pulsar emission may be a violent event that may be revealed by high-energy observations. Although an archival search for x-ray or γ-ray counterparts for PSR B1931+24 has not been successful, the relatively large distance from the pulsar (~4.6 kpc) and arbitrary viewing periods may make such a detection unlikely.

The relation between the presence of pulsar emission via radiating particles and the increased spin-down rate of the neutron star provides strong evidence that a pulsar wind plays a substantial role in the pulsar braking mechanism. Although this has been suggested in the past (*12*), direct observational evidence has been missing so far. As a consequence of the wind's contribution to the pulsar spin-down, magnetic fields estimated for normal pulsars from their observed spin-down rates are likely to be overestimated.

The discovery of PSR B1931+24's behavior suggests that many more such objects exist in the Galaxy but have been overlooked so far because they were not active during either the search or confirmation observations. The periodic transient source serendipitously found recently in the direction of the galactic center (*13*) may turn out to be a short–time-scale version of PSR B1931+24 and hence to be a radio pulsar. In general, the time scales involved in the observed activity patterns of these sources pose challenges for observations scheduled with current telescopes. Instead, future telescopes with multibeaming capabilities, like the Square-Kilometre-Array or the Low Frequency Array, which will provide continuous monitoring of such sources, are needed to probe such time scales, which are still almost completely unexplored in most areas of astronomy.

References and Notes

1. A. G. Lyne, R. N. Manchester, J. H. Taylor, *Mon. Not. R. Astron. Soc.* **213**, 613 (1985).
2. G. H. Stokes, J. H. Taylor, J. M. Weisberg, R. J. Dewey, *Nature* **317**, 787 (1985).
3. G. Hobbs, A. G. Lyne, M. Kramer, C. E. Martin, C. Jordan, *Mon. Not. R. Astron. Soc.* **353**, 1311 (2004).
4. D. C. Backer, *Nature* **228**, 42 (1970).
5. I. H. Stairs, A. G. Lyne, S. Shemar, *Nature* **406**, 484 (2000).
6. F. C. Michel, *Theory of Neutron Star Magnetospheres* (Univ. of Chicago Press, Chicago, 1991).
7. F. Pacini, *Nature* **216**, 567 (1967).
8. J. E. Gunn, J. P. Ostriker, *Nature* **221**, 454 (1969).
9. A. K. Harding, I. Contopoulos, D. Kazanas, *Astrophys. J.* **525**, L125 (1999).
10. D. R. Lorimer, M. Kramer, *Handbook of Pulsar Astronomy* (Cambridge Univ. Press, Cambridge, 2005).
11. P. Goldreich, W. H. Julian, *Astrophys. J.* **157**, 869 (1969).
12. A. Spitkovsky, in *Young Neutron Stars and Their Environments, IAU Symposium 218*, F. Camilo, B. M. Gaensler, Eds. (Astronomical Society of the Pacific, San Francisco, CA, 2004), pp. 357–364.
13. S. D. Hyman *et al.*, *Nature* **434**, 50 (2005).
14. J. M. Cordes, T. J. W. Lazio, *NE2001. I. A New Model for the Galactic Distribution of Free Electrons and Its Fluctuations* (2002). Available at http://xxx.lanl.gov/abs/astro-ph/0207156.

15. D.R.L. is a University Research Fellow funded by the Royal Society.

19 December 2005; accepted 13 February 2006
Published online 23 February 2006;
10.1126/science.1124060
Include this information when citing this paper.

Quantum-Dot Spin-State Preparation with Near-Unity Fidelity

Mete Atatüre,[1]* Jan Dreiser,[1] Antonio Badolato,[1] Alexander Högele,[1,2] Khaled Karrai,[2] Atac Imamoglu[1]*

We have demonstrated laser cooling of a single electron spin trapped in a semiconductor quantum dot. Optical coupling of electronic spin states was achieved using resonant excitation of the charged quantum dot (trion) transitions along with the heavy-light hole mixing, which leads to weak yet finite rates for spin-flip Raman scattering. With this mechanism, the electron spin can be cooled from 4.2 to 0.020 kelvin, as confirmed by the strength of the induced Pauli blockade of the trion absorption. Within the framework of quantum information processing, this corresponds to a spin-state preparation with a fidelity exceeding 99.8%.

Semiconductor quantum dots (QDs) have been referred to as artificial atoms because of their discrete atom-like states. Photoluminescence (PL) studies of single QDs under nonresonant excitation have led to the generation of single photons (*1*, *2*) and cavity-quantum electrodynamics in the weak-coupling (*2*–*4*) and strong-coupling (*5*–*7*) regimes: all indicators of a quantum optical system. Similarly, resonant excitation has enabled the observation of Rabi oscillations (*8*) and coherent manipulation of excitons (*9*). These advances, in turn, have strengthened various proposals, including those regarding optical accessing of spins in QDs (*10*). However, from the perspective of quantum information processing (*11*), the ability to prepare, manipulate, and detect a spin qubit optically in solid-state systems is yet to be demonstrated.

We have demonstrated the high-fidelity preparation of a QD spin state via laser cooling [optical pumping (*12*)]. Using the Pauli blockade strength of the corresponding optical transitions as a means to infer the electron spin state, we showed that spin cooling due to spontaneous spin-flip Raman scattering can dominate over the heating introduced by hyperfine-induced spin-flip or cotunneling events. This allowed us to cool the spin temperature of an electron from 4.2 K (determined by the heat bath) down to 20 mK. By controlling the relative strength of these processes via gate voltage and magnetic field, we can tune the system from the regime of an isolated artificial atom to that of a quantum-confined solid-state system coupled either to a charge or a spin reservoir.

The experiments were performed on molecular-beam-epitaxy–grown single self-assembled InAs/GaAs QDs in a gated heterostructure, where the only difference as compared to the one used in (*13*) was the 35-nm tunnel barrier between the QD layer and the electron reservoir. In similar devices, a gate voltage applied between the ohmic and the Schottky contacts provides deterministic charging of QDs with signatures in the optical transitions (*14*). We performed the initial characterization of our QDs by conventional micrometer-resolution photoluminescence (μ-PL) spectroscopy at 4.2 K to determine the voltage range for each charging state, along with the associated optical transition frequencies. Figure 1A shows a typical gate sweep for our device, and the labels X^0 and X^{1-} identify the relevant optical transitions for our experiments: those from an empty QD and those from a single-electron–charged QD. We then carried out magneto-optical spectroscopy of the X^{1-} transition to extract the excitonic Zeeman splitting of 30 GHz/T. Having characterized the basic optical properties of the QD, we switched to resonant excitation using differential transmission technique: Fig. 1B shows a typical absorption plot at 0 T as a single-frequency laser is tuned across the trion transition. The details of this technique (*15*) along with its advantages in spin-selective measurements (*16*) can be found in previous works.

A single-electron–charged QD in the trion picture is analogous to the four-level system illustrated in Fig. 2A, where state $|\uparrow\downarrow, \blacktriangledown\rangle$ ($|\uparrow\downarrow, \blacktriangle\rangle$) corresponds to the QD with two ground-state electrons forming a singlet and a ground-state hole with angular momentum projection $J_z = -3/2$ (3/2) along the growth direction. The strong trion transitions, $|\uparrow\downarrow, \blacktriangledown\rangle \leftrightarrow |\downarrow\rangle$ and $|\uparrow\downarrow, \blacktriangle\rangle \leftrightarrow |\uparrow\rangle$, leave the resident electron spin unaltered, whereas the weak transitions, $|\uparrow\downarrow, \blacktriangledown\rangle \leftrightarrow |\uparrow\rangle$ and $|\uparrow\downarrow, \blacktriangle\rangle \leftrightarrow |\downarrow\rangle$, lead to a net spin-flip of the resident electron. The latter transitions are ideally forbidden by the optical selection rules; nevertheless, inherent heavy-light hole mixing

[1]Institute of Quantum Electronics, ETH Zurich, CH-8093 Zurich, Switzerland. [2]Center for NanoScience and Sektion Physik, Ludwig-Maximilians-Universität, 80539 Munich, Germany.

*To whom correspondence should be addressed. E-mail: atature@phys.ethz.ch (M.A.); imamoglu@phys.ethz.ch (A.I.)